

See discussions, stats, and author profiles for this publication at: <https://www.researchgate.net/publication/6692852>

# In Situ Flavonoid Analysis by FT-Raman Spectroscopy: Identification, Distribution, and Quantification of Aspalathin in Green Rooibos ( *Aspalathus linearis* )

ARTICLE in ANALYTICAL CHEMISTRY · DECEMBER 2006

Impact Factor: 5.64 · DOI: 10.1021/ac061123q · Source: PubMed

---

CITATIONS

28

---

READS

78

## 4 AUTHORS, INCLUDING:



**Malgorzata Baranska**

Jagiellonian University

159 PUBLICATIONS 1,870 CITATIONS

SEE PROFILE



**Hartwig Schulz**

Julius Kühn-Institut

178 PUBLICATIONS 2,218 CITATIONS

SEE PROFILE



**Elizabeth Joubert**

Agricultural Research Council, South Africa

158 PUBLICATIONS 2,999 CITATIONS

SEE PROFILE

# In Situ Flavonoid Analysis by FT-Raman Spectroscopy: Identification, Distribution, and Quantification of Aspalathin in Green Rooibos (*Aspalathus linearis*)

Malgorzata Baranska,<sup>†,‡</sup> Hartwig Schulz,<sup>\*,†</sup> Elizabeth Joubert,<sup>§,||</sup> and Marena Manley<sup>||</sup>

Federal Centre for Breeding Research on Cultivated Plants, Institute of Plant Analysis, Neuer Weg 22-23, D-06484 Quedlinburg, Germany, Faculty of Chemistry, Jagiellonian University, Ingardena 3, 30-060 Cracow, Poland, ARC Infruitec-Nietvoorbij, Private Bag X5026, Stellenbosch, 7599, South Africa, and Department of Food Science, Stellenbosch University, Private Bag X1, Matieland (Stellenbosch), 7602, South Africa

FT-Raman spectroscopy was used for the first time for in situ identification of aspalathin and quantification of the dihydrochalcones in dried, green rooibos (*Aspalathus linearis*). With the support of two-dimensional correlation spectroscopy, characteristic key bands of aspalathin, the main flavonoid and antioxidant occurring in rooibos, were localized and identified in the spectra obtained from various plant samples. Application of Raman mapping revealed the spatial distribution of this valuable dihydrochalcone within the intact dried leaves. Based on the spectral data and reference HPLC values, reliable multivariate calibration models were developed for quantification of aspalathin, nothofagin, and the combined dihydrochalcone contents of dried, green rooibos.

Flavonoids are secondary metabolites widely distributed in vascular plants. They belong to the group of phenolic compounds with two aromatic rings, bonded with a central pyran ring, and can be divided into several classes such as flavones, flavonols, flavanonols, flavanones, anthocyanins, flavanols (catechins), and chalcones, based on the oxidation stage of the pyran ring and on the characteristic color. Structures of individual flavonoids differ in their hydroxylation, methylation, acylation, and glycosylation pattern and form a large natural diversity of compounds.<sup>1</sup> They are extensively used in medicines, food, textiles, and cosmetics, either as complex mixtures or pure isolated substances. Quantification of flavonoids in plant material is usually performed by HPLC, which provides high selectivity and accuracy, but this method is also time-consuming and may require sample cleanup. However, for production purposes, often only general plant classification or an approximate determination of flavonoid levels is required. Rapid analysis or screening of raw plant material at an early stage of production is of great interest to identify plant

material with sufficient quantities of valuable compounds. UV–visible spectroscopy and colorimetry can be used as screening methods, however, they also require solvent extraction and trained laboratory personnel and are time-consuming. As an alternative the use of NIR spectroscopy has been considered, which allows prediction of the content of the major phenolic compounds in raw plant material with accuracy acceptable for industry.<sup>2,3</sup> However, other more precise, informative, and fast methods are also of interest.

Recently, FT-Raman spectroscopy has been successfully applied to investigate various secondary plant metabolites, either for quality or quantity analysis.<sup>4–9</sup> The measurements are obtained nondestructively directly from the plant tissue, without the need to isolate the compounds. In this context also, different classes of flavonoids, responsible for plant pigmentation, i.e., anthocyanins and glycosides of flavonols, have been determined in plant tissue (paper in preparation). The present study demonstrates in situ analysis of aspalathin, a dihydrochalcone, which is the major flavonoid occurring in leaves and stems of green (unfermented) rooibos (*Aspalathus linearis*).<sup>10</sup> Present in high quantities, it makes a substantial contribution to the antioxidant capacity of rooibos.<sup>11</sup> The rooibos plant is indigenous to South Africa and increasingly of interest to the nutraceutical and cosmetic industries for development of new products due to its high antioxidant activity.<sup>11–15</sup>

\* To whom correspondence should be addressed. Fax: +49 3946 47234. E-mail: h.schulz@bafz.de.

<sup>†</sup> Institute of Plant Analysis.

<sup>‡</sup> Jagiellonian University.

<sup>§</sup> ARC Infruitec-Nietvoorbij.

<sup>||</sup> Stellenbosch University.

(1) Delgado-Vargas, F.; Jiménez, A. R.; Paredes-López, O. *Crit. Rev. Food Sci. Nutr.* 2000, 40, 173–289.

(2) Manley, M.; Joubert, E.; Botha, M. J. *NIR Spectrosc.* 2006, 14, 213–222.

(3) Joubert, E.; Manley, M.; Botha, M. J. *Agric. Food Chem.* 2006, 54, 5279–5283.

(4) Baranska, M.; Schulz, H.; Siuda, R.; Strehle, M. A.; Rösch, P.; Popp, J.; Joubert, E.; Manley, M. *Biopolymers* 2005, 77, 1–8.

(5) Schulz, H.; Baranska, M.; Quilitzsch, R.; Schütze, W.; Lösing, G. J. *J. Agric. Food Chem.* 2005, 53, 3358–3363.

(6) Baranska, M.; Schulz, H.; Reitzenstein, S.; Uhlemann, U.; Strehle, M. A.; Krüger, H.; Quilitzsch, R.; Foley, W.; Popp, J. *Biopolymers* 2005, 78, 237–248.

(7) Schulz, H.; Baranska, M.; Baranski, R. *Biopolymers* 2005, 77, 212–221.

(8) Baranski, R.; Baranska, M.; Schulz, H. *Planta* 2005, 222, 448–457.

(9) Baranska, M.; Schulz, H.; Baranski, R.; Nothnagel, T.; Christensen, L. J. *Agric. Food Chem.* 2005, 53, 6565–6571.

(10) Joubert, E. *Food Chem.* 1996, 55, 403–411.

(11) Schulz, H.; Joubert, E.; Schütze, W. *Eur. Food Res. Technol.* 2003, 216, 539–543.

(12) Standley, L.; Winterton, P.; Marnewick, J. L.; A. Gelderblom, W. C.; Joubert, E.; Britz, T. J. *J. Agric. Food Chem.* 2001, 49, 114–117.

For production of extracts high in aspalathin content, its concentration in the plant material is the most important factor. A minimum level of 4% for aspalathin in rooibos is required in order to obtain satisfactory enrichment of final dried extracts.<sup>2</sup> In this paper, we demonstrate that FT-Raman spectroscopy fulfills the demand for rapid analysis of the aspalathin content in rooibos in order to identify plants with satisfactory high levels. For the first time, we present the use of FT-Raman spectroscopy for the identification of aspalathin as the main flavonoid compound in dried, green rooibos and the development of a FT-Raman quantification method for prediction of aspalathin, nothofagin, and total dihydrochalcone levels. Additionally, the advantage of two-dimensional (2D) correlation algorithms for reliable band assignment and an improved Raman quality analysis is demonstrated. Furthermore, by using the FT-Raman mapping technique, a spatial distribution of aspalathin in the intact rooibos leaf was also demonstrated.

## EXPERIMENTAL SECTION

**Plant Material and Reference Analysis.** Purified aspalathin (batch A/02) was isolated by Petra Snijman at the PROMEC (Programme on Mycotoxin and Experimental Carcinogenesis) Unit of the Medical Research Council of South Africa (MRC, Bellville, South Africa).

The plant material samples comprised a selection of ground, dried green rooibos plant material ( $n = 100$ ) from the sample set used by Manley et al.,<sup>2</sup> covering the same range for aspalathin content. The sample set included plant material harvested during different years and from different production areas. For in situ determination of the spatial distribution of aspalathin in the intact rooibos leaf, shoots were harvested and dried naturally at room temperature, before the intact leaves were removed from the stems.

Duplicate acetonitrile–water extracts, prepared by extracting ~0.5 g of ground, dried plant material with 15 mL of acetonitrile and 30 mL of deionized water on a steam bath for 15 min, was cooled to room temperature and filled to volume (100 mL) with 1% (w/v) ascorbic acid solution. Each extract was filtered through a Whatman No. 4 filter paper, followed by a Millipore Millex-HV hydrophilic PVDF syringe filter (0.45  $\mu\text{m}$ ; 25-mm diameter) (Microsep (Pty.) Ltd., Bellville, South Africa) directly into an autosampler vial for immediate HPLC analysis. Separation of the extract (10  $\mu\text{L}$ ) was performed in duplicate on a Phenomenex Synergy MAX-RP C12 80 A column (TMS end capping, 4  $\mu\text{m}$ , 150  $\times$  4.5 mm i.d.) (Separations, Johannesburg, South Africa) at 30  $^{\circ}\text{C}$ , using the solvent gradient program of Schulz et al.<sup>11</sup> The LaChrom (Merck/Hitachi) HPLC system comprised an L7000 interface, L7400 UV detector, L7100 pump, L7200 autosampler, and L7450 DAD detector. The DAD detector was used to confirm peak identity. A Phenomenex degasser model DG-4400 (Separations, Cape Town, South Africa) was used to degas solvents in-line. Peak area integration of measurements at 288 nm was done with the LaChrom Multisystem Software D700. A standard series

of aspalathin (concentration range 0.08–4.0  $\mu\text{g}$  injected;  $R^2 > 0.99$ ) was used to calculate the aspalathin content, and an absorbance ratio in terms of aspalathin was used to calculate the nothofagin content. The sum of aspalathin and nothofagin contents was expressed as “total dihydrochalcone content” of the plant material.

**FT-Raman Measurements.** Raman spectra of dried, intact leaves and dried, ground samples, containing either only leaves or a mixture of leaves and stems, were recorded using a Bruker NIR-FT-Raman spectrometer (model RFS 100) equipped with a Nd:YAG laser, emitting at 1064 nm, and a germanium detector cooled with liquid nitrogen. The instrument was equipped with a flat  $x$ – $y$  stage, a mirror objective, and a prism slide for redirection of the laser beam. In contrast to the standard vertical sampling arrangement, the samples were mounted horizontally. Longitudinal and transverse sections of rooibos leaves were used for Raman mapping, whereas ground samples were used for single spectral measurements. Samples were placed on the stage as-is and exposed to the laser beam of ~0.1-mm diameter. All spectra were measured in the range from 100 to 4000  $\text{cm}^{-1}$  with 150-mW laser power and spectral resolution of 4  $\text{cm}^{-1}$ ; 256 scans were collected for single measurements whereas mappings were performed with 4 scans per each point with a spatial resolution of 30 and 200  $\mu\text{m}$ , for transverse and longitudinal sections of the intact leaves, respectively. The spectra were processed using the OPUS/map software package v. 4.3 (Bruker GmbH) and background corrected prior to analysis.

**Two-Dimensional Correlation Analysis.** Synchronous and asynchronous Raman spectra were calculated by using the algorithm developed by Noda and Ozaki<sup>16</sup> included in the OPUS software. A set of seven selected spectra was arranged in increasing order of aspalathin content. Data pretreatment (multiplicative scatter correction (MSC), smoothing, and baseline correction (BC)) was performed using the same software.

**Development of Calibration Statistics.** Chemometric analyses of the Raman spectra were performed using the chemometrics software package GRAMS 7.0 (Galactic Ind., Salem, MA). Pretreatments, evaluated to transform the spectral data, were Multiple Scatter Correction (MSC), standard normal variate (SNV), vector normalization (VN), and Baseline Correction (BC). The data were subsequently mean centered. Selected wavenumber ranges, as well as the full recorded spectral range, were evaluated for development of partial least-squares (PLS) calibration models for the individual compounds, i.e., aspalathin and nothofagin, as well as the total dihydrochalcone content, respectively. Outlier samples were eliminated from the data set. Statistical accuracy was described by means of the coefficient of determination ( $R^2$ ) and the standard error of cross validation (SECV). The optimum number of PLS factors for each component was determined by application of the PRESS (predictive residual error sum of squares) calculation.

## RESULTS AND DISCUSSION

**Identification of Flavonoids in Plant Material.** Rooibos flavonoids predominantly consist of dihydrochalcones, flavonols, and flavones, with aspalathin (Figure 1) as the main polyphenol in unfermented plant material. The dihydrochalcone aspalathin

(13) von Gadow, A.; Joubert, E.; Hansmann, C. F. *J. Agric. Food Chem.* **1997**, *45*, 632–638.

(14) Joubert, E.; Winterton, P.; Britz, T. J.; Ferreira, D. *Food Res. Int.* **2004**, *37*, 133–138.

(15) Joubert, E.; Winterton, P.; Britz, T. J.; Gelderblom, W. C. A. *J. Agric. Food Chem.* **2005**, *53*, 10260–10267.

(16) Noda, I.; Ozaki, Y. *Two dimensional correlation spectroscopy: applications in vibrational and optical spectroscopy*; J. Wiley & Sons: Chichester, 2004.

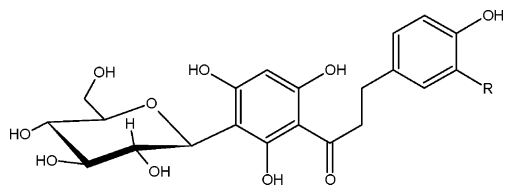


**Figure 1.** Structure of aspalathin (R = OH) and nothofagin (R = H) occurring in rooibos (*A. linearis*)

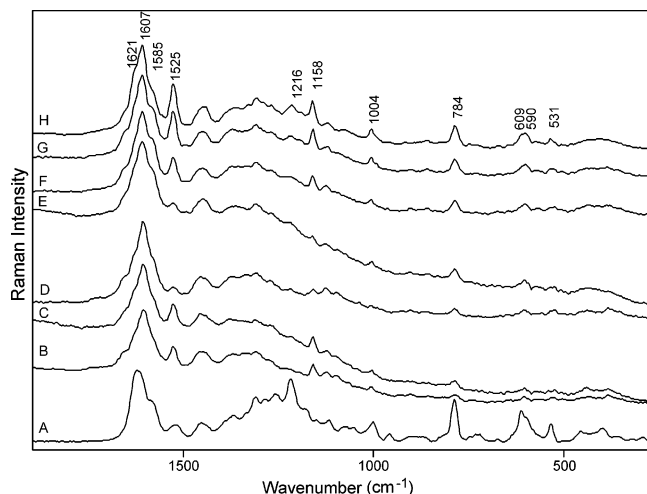


**Figure 2.** FT-Raman spectrum of pure, isolated aspalathin (A) and a set of spectra obtained from ground, dried, green rooibos plant material samples containing 1.86 (B), 2.15 (C), 3.31 (D), 3.75 (E), 4.46 (F), 6.38 (G), and 13.08% (H) aspalathin. Bands observed at 1525, 1158, and 1004  $\text{cm}^{-1}$  can be assigned to carotenoids.

is unique, species-specific,<sup>10,17</sup> and until now it has only been isolated from rooibos. Nothofagin, similar in structure to aspalathin except for the degree of hydroxylation of the B-ring (Figure 1), is the second most important polyphenol in rooibos.<sup>10</sup>

A Raman spectrum obtained from pure, isolated aspalathin (A), as well as selected spectra from ground, dried green rooibos samples, sequenced according to increasing aspalathin content (B–H), is presented in Figure 2. Rooibos spectra show characteristic bands of carotenoids at 1525, 1158, and 1004  $\text{cm}^{-1}$ . The distinctive characteristic of carotenoid structure is a long central chain with a conjugated double-bond system, which is a light-absorbing chromophore responsible for the color of these compounds. Although these natural pigments occur in plants as minor components, a very sensitive detection can be achieved by NIR-FT-Raman spectroscopy, which gives a strong enhancement of carotenoids due to the known preresonance effect.<sup>18</sup> Carotenoid bands observed in the Raman spectrum at 1525 and 1158  $\text{cm}^{-1}$  can be assigned to in-phase C=C ( $\nu_1$ ) and C–C stretching ( $\nu_2$ ) vibrations of the polyene chain, respectively. Additionally, in-plane rocking mode of  $\text{CH}_3$  groups attached to the polyene chain and coupled with C–C bonds are seen at 1004  $\text{cm}^{-1}$ .<sup>7,8,19</sup> It has been shown that the wavenumber location of these bands,<sup>19</sup> and in particular the  $\nu_1$  band, is strongly dependent on the length of the carotenoid chain, and generally, carotenoids with 11,9,8,7-

conjugated C=C bonds have their characteristic bands at about 1510, 1524, 1530, and 1536  $\text{cm}^{-1}$ .<sup>7,8</sup> This band can be used for identification purposes, although their wavenumber can be slightly influenced by carotenoid side groups and bonding to other plant constituents. Raman signals of carotenoids seen in the rooibos spectra at 1525  $\text{cm}^{-1}$  (Figure 2) indicate that those pigments possess nine conjugated C=C bonds in their backbone.

Some spectral features of aspalathin are also clearly observed, and especially the lower frequency range shows signals at approximately 780, 600, and 530  $\text{cm}^{-1}$ , of which the intensities increase with higher concentrations of aspalathin. It can therefore be assumed that these vibrational modes represent key bands of this dihydrochalcone.

Merlin et al.<sup>20–22</sup> have investigated anthocyanins using resonance Raman (RR) spectroscopy and showed a strong influence of glycosylation on the benzopyrylium part of the flavonoid molecule (rings A and C). Some characteristic spectral features of this phenomenon were provided; i.e., monoglycosides (in position 3 of the C ring) exhibit a strong RR signal close to 540  $\text{cm}^{-1}$ , while 3,5-diglycosides have a stronger signal in the higher frequency range close to 630  $\text{cm}^{-1}$ . In the case of aspalathin, monoglycosylation corresponds to carbon-5 of the A ring of anthocyanins. The characteristic band at  $\sim 530 \text{ cm}^{-1}$  (Figure 2) can therefore be associated with the presence of the glucose moiety of the aspalathin molecule. This signal is clearly observed in the FT-Raman spectra obtained from pure aspalathin, as well as from the plant material (Figure 2).

Signals at 784 and 609  $\text{cm}^{-1}$  in the aspalathin spectrum correspond to out-of-plane C–H deformation of the phenyl rings. The other characteristic band at 1216  $\text{cm}^{-1}$  can be assigned to hydroxyl deformation and ring vibration; however, it overlaps slightly with other signals of the rooibos plant matrix.

The most intensive bands of aspalathin in the range 1550–1670  $\text{cm}^{-1}$ , due to the phenyl rings and C=O stretching vibrations (carbonyl vibration occurs at an untypically low wavenumber due to coupling with the aroma ring),<sup>6</sup> coincide to a large extent in the rooibos spectra, hampering detailed interpretation. Even a spectrum, obtained from a sample containing exceptionally high amounts of aspalathin ( $\sim 13\%$ ) (Figure 2H), presents broad, overlapping bands in this range, resulting in ambiguous identification. Therefore, to establish a correct interpretation, generalized 2D correlation spectroscopy was applied. This technique has already been applied to various types of spectroscopy and materials, including investigations of biological samples, e.g., wheat, milk, and chicken meat.<sup>23–25</sup> One special advantage of 2D correlation analysis is simplification of complex spectra, consisting of many overlapping peaks, and enhancement of spectral resolution by spreading spectral peaks over the second dimension. Furthermore, unambiguous assignment through correlation of bands can be established.<sup>16,26</sup>

(20) Merlin, J.-C.; Statoua, A.; Cornard, J.-P.; Saidi-Idrissi, M.; Brouillard, R. *Phytochemistry* **1994**, *35*, 227–232.

(21) Merlin, J.-C.; Statoua, A.; Brouillard, R. *Phytochemistry* **1985**, *24*, 1575–1581.

(22) Merlin, J.-C.; Cornard, J. P. *Spectrochim. Acta, A* **1994**, *50*, 703–712.

(23) Archibald, D. D.; Kays, S. E.; Himmelsbach, D. S.; Barton, F. E., II. *J. NIR Spectrosc.* **1996**, *4*, 139–152.

(24) Czarnik-Matusewicz, B.; Murayama, K.; Tsenkova, R.; Ozaki, Y. *Appl. Spectrosc.* **1999**, *53*, 1582–1594.

(25) Liu, Y.; Barton II, F. E.; Lyon, B. G.; Chen, Y.-R. *J. NIR Spectrosc.* **2003**, *11*, 457–466.

(17) Marnewick, J. L.; Joubert, E.; Swart, P.; van der Westhuizen, F.; Gelderblom, W. C. *J. Agric. Food Chem.* **2003**, *51*, 8113–81119.

(18) Ozaki, Y.; Cho, R.; Ikegawa, K.; Muraishi, S.; Kawauchi, K. *Appl. Spectrosc.* **1992**, *46*, 1503–1507.

(19) Withnall, R.; Chowdhry, B. Z.; Silver, J.; Edwards, H. G. M.; de Oliveira, L. F. C. *Spectrochim. Acta, A* **2003**, *59*, 2207–2212.



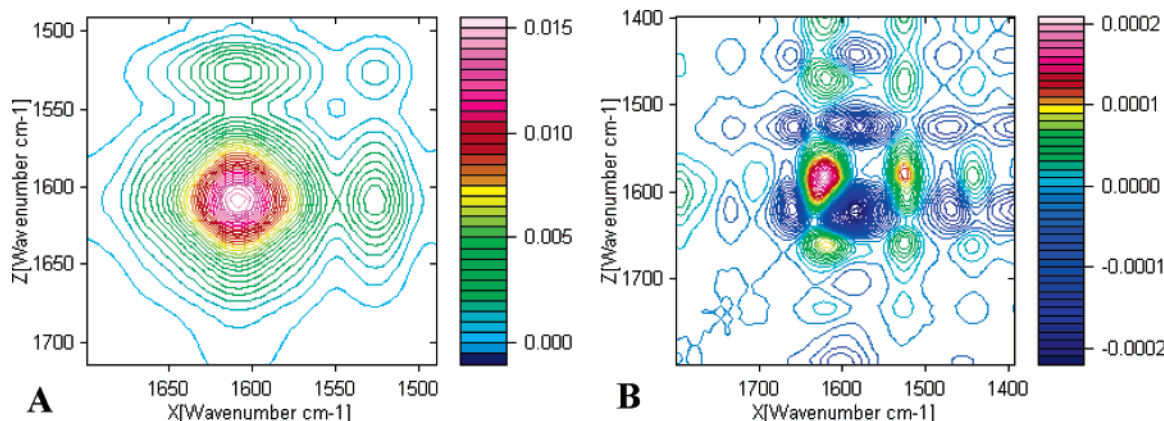


**Figure 3.** Synchronous (A) and asynchronous (B) 2D correlation spectra of rooibos.

The application of generalized 2D correlation analysis of rooibos samples was challenging, as most materials so far investigated by this method were rather simple, often synthetically prepared, and consisted of one or two components. The plant material investigated in this study contained various compounds such as carotenoids, flavonoids, and lignin and presented large variability with regard to composition between samples. However, for 2D correlation analysis, a set of samples with known, increasing concentration of aspalathin was selected, which was used as an external perturbation for creating synchronous and asynchronous spectra. Their countermaps in the range 1800–1400  $\text{cm}^{-1}$ , constructed from the set of seven spectra after pretreatment, are presented in Figure 3A and B, respectively. Autopeaks, observed in the synchronous spectrum, should indicate bands of which intensities vary most significantly with increasing concentration of aspalathin in rooibos samples. However, a broad autopeak at  $\sim 1610 \text{ cm}^{-1}$  could not be unambiguously assigned to one rooibos component. In this range, signals occurred due to aspalathin, but could also be attributed to other plant matrix constituents (e.g., lignin).<sup>27</sup> More information is provided by asynchronous 2D correlation map, which develops a large number of peaks. A clear symmetric cluster pattern, comprising two positive and two negative cross peaks, can be observed. The vertical pair is asynchronous cross peaks is positive and the horizontal pair negative, so the observed pattern is associated with the process of line broadening. This indicates that an increase in aspalathin content in the rooibos samples results in an expansion of the band near  $1610 \text{ cm}^{-1}$ . It must therefore be associated with higher intensities of those bands assigned to aspalathin, occurring below and above  $1610 \text{ cm}^{-1}$ . The analysis of changes in intensity in the asynchronous map can be simplified by extracting a slice spectrum. The 2D slice spectrum may provide information regarding the resolution enhancement of bands and the order of the changes in intensity between one particular band and others observed. Figure 4 shows a slice spectrum at  $1585 \text{ cm}^{-1}$ , a position characteristic for one of the signals of aspalathin. Other plant matrix vibrations are usually not observed at this wavenumber. The observed peaks in this slice at approximately 1620, 1580, and  $1520 \text{ cm}^{-1}$  are not present (or are obscured) in the corresponding synchronous map shown in Figure 3A. This results from the fact

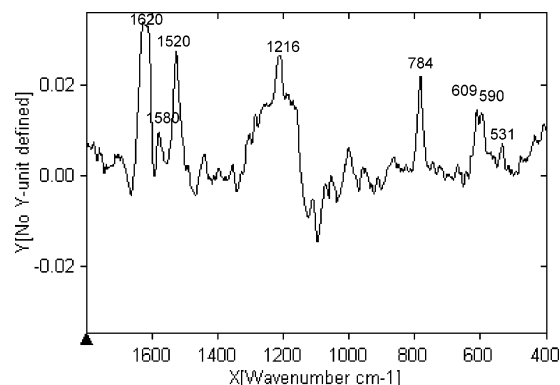


**Figure 4.** Slice spectrum along  $1585 \text{ cm}^{-1}$  line in the asynchronous spectrum shown in Figure 3B.

that asynchronous correlation spectra have more powerful deconvolution ability for highly overlapping bands.<sup>24</sup> Therefore, the asynchronous spectrum correlated with changes in one of the aspalathin bands detects other peaks corresponding to this band. The slice performed at  $1585 \text{ cm}^{-1}$  resembles the spectrum of pure aspalathin (distinct bands at 1216 and  $531 \text{ cm}^{-1}$  and doublet at 609 and  $590 \text{ cm}^{-1}$ ), confirming that the observed changes in the intensity of those bands are strongly correlated with the increase in concentration of this dihydrochalcone.

The most characteristic vibrational frequencies and their tentative assignments for aspalathin are presented in Table 1.

**Distribution of Aspalathin.** It has been demonstrated before that RR microspectrometry can be used for studying anthocyanins in the plant matrix;<sup>20</sup> however, using this method, the vibrational modes of the benzopyrylium moiety can be recorded rather than any other spectral features of the remainder of these molecules. Using FT-Raman mapping, it is possible not only to identify the analyzed component but also to investigate its distribution in the intact plant tissue.

Figure 5 presents Raman maps obtained from transverse (A) and longitudinal (B) sections of a dried, intact rooibos leaf, colored according to the intensity of the signal at  $784 \text{ cm}^{-1}$ , which has been identified previously as the key band for aspalathin. From these results it can clearly be seen that this valuable compound is distributed heterogeneously in the sample and the highest concentration was observed in the inner part of the leaves. Simultaneously, it is possible to integrate other bands, e.g., the

(26) Noda, I. *Vibr. Spectrosc.* **2004**, *36*, 143–165.

(27) Gierlinger, N.; Schwanninger, M. *Plant Physiol.* **2006**, *140*, 1246–1254.

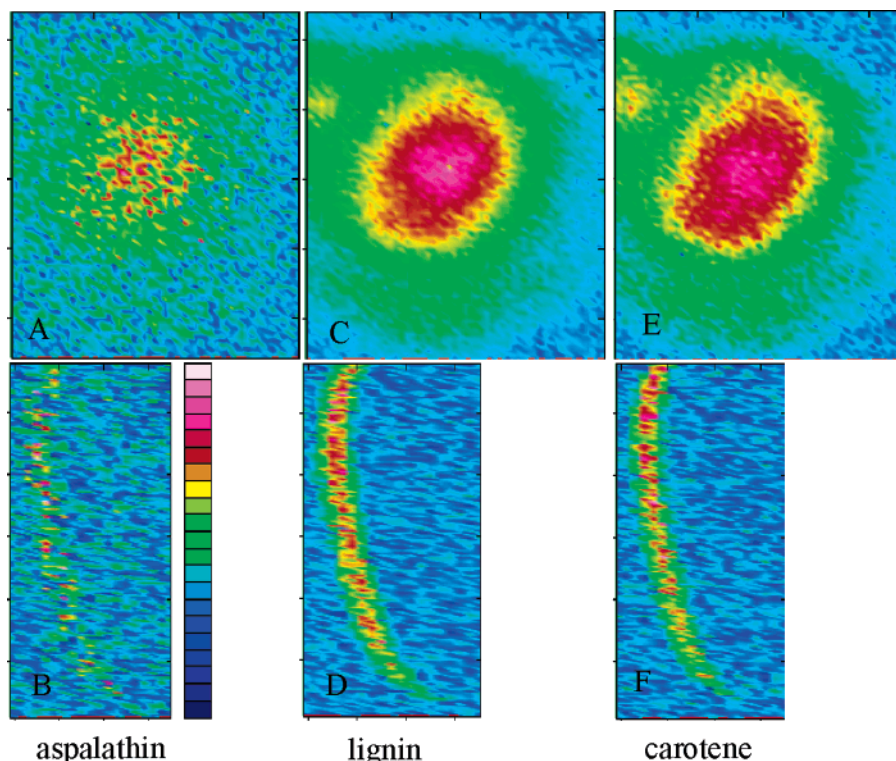


**Figure 5.** Raman maps obtained from transverse (A, C, E) and longitudinal sections of rooibos leaves (B, D, F) colored according to the individual band intensities at 784 (A, B), 1607 (C, D), and 1525  $\text{cm}^{-1}$  (E, F) showing the relative content of aspalathin, lignin, and carotenoids, respectively. (mapping parameters: (A, C, E) area  $1700 \times 2500 \mu\text{m}$ , increment  $30 \mu\text{m}$ ; (B, D, F) area  $3700 \times 28700 \mu\text{m}$ ; increment  $200 \mu\text{m}$ ).

**Table 1. Characteristic Vibrational Bands and Their Tentative Assignment for Aspalathin**

wavenumber ( $\text{cm}^{-1}$ )	relative intensities	assignment
3060	23	aromatic (C–H) stretch
3034	17	aromatic (C–H) stretch
2924	100	aliphatic (C–H) stretch
1621	91	ring stretches
1585 sh <sup>a</sup>	39	(C=O) stretch
1518	16	ring stretch
1452	24	$\text{CH}_2$ deformation
1216	59	(O–H) deformation + ring vibration
999	12	ring “breathing”
784	27	aromatic (C–H) out-of-plane deformation
609	25	aromatic (C–H) out-of-planed deformation
590	14	rings deformation
531	9	glucose moiety (C–C) deformation

<sup>a</sup> sh-shoulder.

signal at  $1607 \text{ cm}^{-1}$ , mainly due to lignin (Figure 5C and D), and the signal at  $1525 \text{ cm}^{-1}$ , showing the distribution of carotenoids (Figure 5E and F). These results demonstrate the advantage of FT-Raman over RR spectroscopy, since fluorescence of the plant matrix does not interfere with the spectra obtained, and several plant components can be simultaneously investigated. The mapping technique also provides information concerning the distribution of the investigated compounds.

**Quantification.** The aspalathin and nothofagin contents of the ground, dried, green rooibos samples used to develop the PLS calibration model, ranged between  $0.59$  and  $10.59 \text{ g/100 g}$  (mean  $\pm$  SD,  $4.15 \pm 2.3$ ) and between  $0.067$  and  $1.23 \text{ g/100 g}$  (mean  $\pm$

**Table 2. FT-Raman Calibration Results for Aspalathin, Nothofagin, and Total Dihydrochalcone Content (TDHC) of Dried, Green Rooibos (*A. linearis*) Plant Material**

	aspalathin	nothofagin	DHC
range (g/100 g)	0.59–10.59	0.067–1.23	0.66–11.83
mean $\pm$ SD	$4.15 \pm 2.3$	$0.50 \pm 0.3$	$4.65 \pm 2.6$
$R^2$	0.83	0.78	0.84
SECV	0.94	0.14	1.04
no. of PLS factors	9	9	9

SD,  $0.50 \pm 0.3$ ), respectively (Table 2). A PLS calibration model was also developed for the total dihydrochalcone (TDHC) content ranging between  $0.66$  and  $11.83 \text{ g/100 g}$  (mean  $\pm$  SD,  $4.65 \pm 2.6$ ). Evaluation of selected wavenumber ranges and the full spectrum indicated that the best PLS calibration models were obtained when the full spectrum was used. The calibration model for the prediction of the aspalathin content was not improved when only aspalathin key bands were selected for development of the PLS model. This finding is in correspondence with studies performed earlier<sup>28</sup> as the PLS regression method is a so-called “full spectrum method” and the calibration model is improved with an increasing number of data points. If the quality of the spectra is not good enough, due to spectral noise or additional compounds in the samples, it may degrade the PLS model. The spectra showed an elevated background, but appropriate data pretreatment allowed the development of reliable calibration models. Data pretreatment

(28) Baranska, M.; Schulz, H.; Walter, A.; Rösch, P.; Quilitzsch, R.; Lösing, G.; Popp, J. *Vibr. Spectrosc.* doi: 10.1016/j.vibspec.2006.08.004.

consisted of VN and BC subsequently mean centered, which successfully removed the side effect of light scattering and variation in particle size. Other pretreatments, i.e., MSC and SNV, did not give calibration results as good as the combination of VN and BC. Three outliers were removed from the data set. The results of the respective PLS calibration models are presented in Table 2.

An FT-Raman calibration model with  $R^2 = 0.83$  (SECV = 0.94) was obtained for the aspalathin content, which was slightly better than a previously obtained calibration model based on NIR spectroscopy measurements ( $R^2 = 0.76$ ; SECV = 0.65).<sup>11</sup> The latter calibration model used a limited concentration range for aspalathin (~4–10 g/100 g of plant material). Using an extended sample set ( $n = 227$ ), with a similar range of aspalathin content (0.60–10.59 g/100 g of plant material) as for the FT-Raman calibration model and an independent validation, resulted in  $R^2 = 0.87$  (SEP = 0.53 g/100 g).<sup>2</sup> The FT-Raman calibration model for nothofagin, present in small amounts in dried, green rooibos (0.067–1.23 g/100 g), shows a relatively high  $R^2 = 0.78$  (SECV = 0.14 g/100 g), taking into consideration the low amounts of this flavonoid present in the samples. Calibration for the total dihydrochalcone content resulted in  $R^2 = 0.84$  (SECV = 1.04 g/100 g). NIR spectroscopy measurements performed on the extended samples set ( $n = 227$ ) gave  $R^2 = 0.77$  (SEP = 0.10 g/100 g) and  $R^2 = 0.88$  (SEP = 0.57 g/100 g) for nothofagin and dihydrochalcone contents, respectively.<sup>2</sup> This illustrates that the main flavonoid

components of dried, green rooibos can be successfully determined by FT-Raman spectroscopy.

## CONCLUSIONS

FT-Raman spectroscopy applied for analysis of dried, green rooibos plant material, assisted by 2D correlation analysis and chemometrics, resulted in calibration models with satisfactory coefficients of determination for the two main flavonoids and comparable to that obtained by NIR spectroscopy. Two-dimensional correlation spectroscopy can support quality analysis by simplifying the complex spectra consisting of many overlapped peaks and enhancing the spectral resolution by spreading spectral peaks over the second dimension. The special advantage of FT-Raman, that several plant components can be simultaneously investigated, was demonstrated. The mapping technique provided information concerning the distribution of aspalathin in the plant tissue.

## ACKNOWLEDGMENT

This work was supported by the Deutsche Forschungsgemeinschaft (DFG), Bonn, Germany (grant Schu 566/7-2), the Raps Foundation, Freising, Germany, and the National Research Foundation (NRF), South Africa.

Received for review June 21, 2006. Accepted August 30, 2006.

AC061123Q